

Suspending superconducting qubits by silicon micromachining F

Cite as: Appl. Phys. Lett. **109**, 112601 (2016); <https://doi.org/10.1063/1.4962327>

Submitted: 10 June 2016 . Accepted: 27 July 2016 . Published Online: 12 September 2016

Y. Chu , C. Axline , C. Wang , T. Brecht , Y. Y. Gao, L. Frunzio, and R. J. Schoelkopf

COLLECTIONS

F This paper was selected as Featured



View Online



Export Citation



CrossMark

ARTICLES YOU MAY BE INTERESTED IN

[Surface participation and dielectric loss in superconducting qubits](#)

Applied Physics Letters **107**, 162601 (2015); <https://doi.org/10.1063/1.4934486>

[Planar superconducting resonators with internal quality factors above one million](#)

Applied Physics Letters **100**, 113510 (2012); <https://doi.org/10.1063/1.3693409>

[Reducing intrinsic loss in superconducting resonators by surface treatment and deep etching of silicon substrates](#)

Applied Physics Letters **106**, 182601 (2015); <https://doi.org/10.1063/1.4919761>



**THE WORLD'S RESOURCE FOR
VARIABLE TEMPERATURE
SOLID STATE CHARACTERIZATION**



OPTICAL STUDIES SYSTEMS



SEEBECK STUDIES SYSTEMS



MICROPROBE STATIONS



HALL EFFECT STUDY SYSTEMS AND MAGNETS

WWW.MMR-TECH.COM

Suspending superconducting qubits by silicon micromachining

Y. Chu,^{a)} C. Axline, C. Wang, T. Brecht, Y. Y. Gao, L. Frunzio, and R. J. Schoelkopf
 Department of Applied Physics, Yale University, New Haven, Connecticut 06511, USA

(Received 10 June 2016; accepted 27 July 2016; published online 12 September 2016)

We present a method for relieving aluminum 3D transmon qubits from a silicon substrate using micromachining. Our technique is a high yield, one-step deep reactive ion etch that requires no additional fabrication processes and results in the suspension of the junction area and edges of the aluminum film. The drastic change in the device geometry affects both the dielectric and the flux noise environment experienced by the qubit. In particular, the participation ratios of various dielectric interfaces are significantly modified, and suspended qubits exhibited longer T_1 's than non-suspended ones. We also find that the suspension increases the flux noise experienced by tunable SQUID-based qubits. *Published by AIP Publishing.* [<http://dx.doi.org/10.1063/1.4962327>]

The coherence times of superconducting qubits have steadily increased over the past decade due to careful engineering of the electromagnetic environment, better materials and fabrication methods, and improved device designs that minimize loss. State-of-the-art superconducting qubits with the longest lifetimes (T_1) make use of very low loss tangent dielectric substrates and have large separation between planar conductors to decrease the effect of dielectric loss in the interfaces between materials.^{1–3} In particular, it has been shown that for aluminum 3D transmons on sapphire, T_1 times are limited by the various interfaces between the dielectric substrate, the superconducting metal, and vacuum.⁴ This effect can be attributed to the larger electric fields near metallic surfaces and the higher concentration of two-level systems (TLS) at disordered interfaces.^{5–7} At the same time, magnetic impurities at the surface of superconductors have been proposed as the cause of $1/f$ flux noise that limits the performance of SQUID based qubits and sensors.^{8–10}

In order to better understand these effects, one strategy is to drastically alter the geometry of materials and interfaces that contribute to qubit loss and decoherence. In this letter, we present a procedure for removing the substrate and suspending aluminum Josephson junctions on silicon by micromachining. Silicon is a low-loss dielectric that offers several advantages for implementing the next generation of complex quantum circuits.^{11,12} Its prevalent use in the semiconductor and MEMS industries have led to a large variety of fabrication techniques that are not available for sapphire.¹³ Using silicon as a substrate material enables the development of novel devices and architectures in circuit QED, such as multilayer quantum circuits that incorporate micromachined superconducting enclosures and resonators.^{14,15} Substrate micromachining has also been used to reduce dielectric loss and frequency noise in niobium titanium nitride coplanar waveguide resonators on silicon.^{16,17} On the other hand, silicon has a more complex surface chemistry than sapphire; for example, it forms an amorphous oxide layer that may be host to a large number of TLS's and paramagnetic impurities.^{11,18,19}

We suspend our qubits with a simple, one-step deep reactive ion etch (DRIE) using the BOSCH process that does

not require any additional steps to mask or protect the devices.^{16,20} We begin with high resistivity (100) silicon wafers ($\rho > 10^4 \Omega \text{cm}$) and fabricate aluminum 3D transmon qubits using the standard Dolan bridge double-angle deposition technique.²¹ DRIE is then performed directly on the fabricated qubits. This is possible because aluminum itself is an excellent mask for the BOSCH process. We have performed this process on more than one hundred devices of various geometries and found that the Josephson junctions were almost all unaffected except for a slight increase in the normal state resistance, possibly due to increased diffusion of the junction oxide when the devices are heated by the etching process.

Figure 1 shows a schematic drawing and scanning electron micrographs (SEM) of suspended 3D transmons. We note that all regions $\sim 700 \text{nm}$ from the edge are undercut,

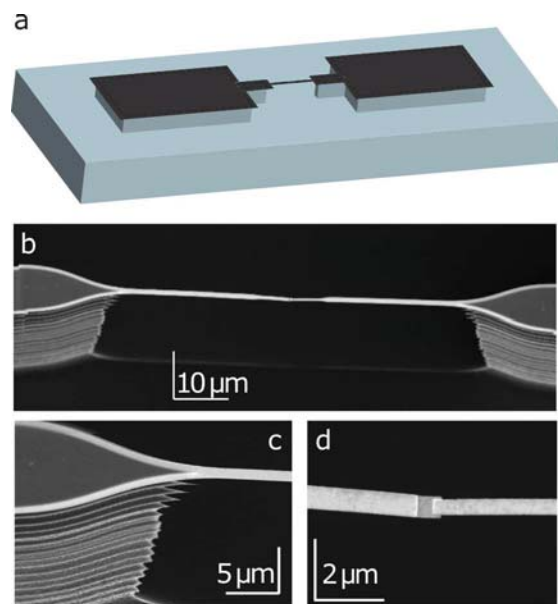


FIG. 1. Micromachined 3D transmons using DRIE. (a) A schematic drawing of a suspended 3D transmon on silicon. An overhang is created at the edges of the metal, while thin features are suspended. (b) SEM image of a BOSCH etched transmon showing the entire suspended leads around the junction region (c) Detailed view of the supporting silicon pedestals, showing the lighter-colored overhanging Al edges and corrugated BOSCH profile. (e) Detailed view of the completely suspended Al-AIO_x-Al Josephson junction.

^{a)}Electronic mail: yiwen.chu@yale.edu

resulting in the junction region and the narrow $1\ \mu\text{m}$ wide leads on either side becoming completely suspended. This means that our process is compatible with aluminum based devices of any geometry, as long as suspended metal regions are supported by other larger features. The suspended single junction transmons are robust against solvent cleaning, drying, and repeated thermal cycles. We observe, however, that more complex suspended structures such as SQUID loops are more easily damaged, for example, by surface tension during solvent cleaning or wet etches.

We first study the effect our process has on dielectric loss and qubit T_1 . Following the analysis in Wang *et al.*,⁴ we quantify the loss due to various dielectric materials using their participation ratios and loss tangents ($\tan\delta$). In Figure 2, we plot the measured T_1 's of several types of qubits with different designs and fabrication procedures against the simulated participation ratios of their metal-substrate (MS) interfaces. Similar plots of T_1 versus the substrate-air (SA) and metal-air (MA) participation ratios can be found in the [supplementary materials](#). In addition to qubits of the design shown in Figure 1 (Design A), we also fabricated a set of qubit designs with higher surface participation (Designs B and C). Design C qubits have planar capacitors whose gaps can be varied to change the surface participations. Drawings of all qubit designs can be found in the [supplementary materials](#). The dielectric participation ratios were obtained through electromagnetic simulations that faithfully modeled the device geometries, including the undercut at the edge of suspended devices.⁴

Without any kind of surface preparation before or after aluminum deposition, the typical T_1 's of the Design A qubits are only a few microseconds, which is more than an order of magnitude worse than the same design on sapphire. The use of surface treatment techniques such as buffered oxide etch (BOE) or oxygen plasma ashing (OPA)²² improves the lifetimes of the regular non-suspended qubits. DRIE further improves the T_1 's of the Design A qubits. The highest T_1

measured with this procedure was $\sim 63\ \mu\text{s}$ for an etch depth of $60\ \mu\text{m}$, which is comparable to the T_1 's of typical qubits of the same design on sapphire. We note that the qubit loss is likely frequency dependent because of coupling to resonant loss channels such as TLS's. This can lead to low T_1 's in exceptional cases, which we have also included in Figure 2. We will explore this further in our later discussion of flux tunable qubits.

The results in Figure 2 indicate that the qualities of interfaces of qubits on silicon are highly dependent on surface treatments and are generally higher loss than those on sapphire. The T_1 's of non-suspended Design A qubits suggest that the surface treatment before and after deposition is important on silicon. On the other hand, only OPA before deposition is needed to obtain $>50\ \mu\text{s}$ T_1 's on sapphire.⁴ It is possible that, for example, the liftoff process leaves more resist residue on silicon than on sapphire. In addition, any exposed silicon surface will form an oxide even after cleaning. Both resist and oxide are likely to result in a higher loss SA interface, which has comparable participation ratios as the MS interface for non-suspended qubits. This may explain the observation that while qubit T_1 's are better after surface cleaning, they never reach the levels measured on sapphire.

It is also evident from Figure 2 that it is insufficient to consider a simple model where qubit loss is dominated by single dielectric interface. The qubits with high MS participation (Design C) have T_1 's that follow a line of constant MS $\tan\delta = 6 \times 10^{-3}$, consistent with being limited by loss due to that interface. However, qubits with lower MS participation (Designs A and B) deviate from that line. One simple explanation for this trend is that the bulk dielectric loss for our silicon substrates becomes significant once the MS participation has been sufficiently reduced. The bulk dielectric participations of the measured qubits, including the suspended ones, are all similar to within 10%. Therefore, we can indicate the T_1 limit due to bulk dielectric loss as a horizontal line in Figure 2. We find that taking into account both bulk and MS surface loss mechanisms results in a model that is consistent with data from both the suspended qubits and the regular qubits that underwent OPA.

We emphasize, however, that other loss mechanisms can play a role as well. For example, the SA and MA participations scale similarly to the MS participation for the regular, non-suspended qubits.⁴ However, unlike a change in qubit geometry, the DRIE process affects the three interfaces differently. In particular, it increases both the SA and MA participations. Therefore, increased loss from the SA and MA interfaces could contribute to negating the T_1 improvement expected from the reduced MS participation. We also cannot rule out more complex effects of the DRIE, such as a change in the SA and MA $\tan\delta$'s from damage or polymer deposition on these surfaces. Furthermore, it is unclear if and how suspension affects other limitations on qubit T_1 , such as loss in the near-junction region, quasiparticles, and phonon coupling.^{4,23,24} Clearly, more investigations are needed to isolate and understand these different effects. Our results indicate that micromachining is a useful technique to alter the loss contributions of various materials in ways not possible with changes in geometry alone. This can help us gain

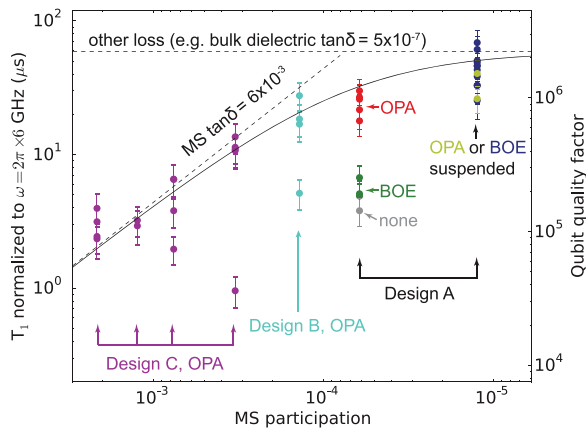


FIG. 2. Lifetime of silicon transmons vs. metal-substrate participation ratio. Each point corresponds to one measured qubit. The MS participation of design C qubits was varied by changing planar capacitor gap distance. The label OPA signifies oxygen plasma ashed before and after deposition, while BOE signifies buffered oxide etch before deposition only. Errorbars are typical variation of T_1 's over time. Dashed lines are guides to the eye corresponding MS surface loss and other effects that are independent of MS participation, such as bulk dielectric loss. Solid line indicates the combination of these loss mechanisms.

information about the roles of these materials in limiting qubit T_1 's.

In order to investigate the effects of DRIE on qubit behavior in more detail, we also measured frequency dependence of the T_1 and flux noise of regular and suspended tunable SQUID qubits. The qubit design is exactly the same as that in Figure 1, except that the single junction is replaced by a $10\ \mu\text{m} \times 10\ \mu\text{m}$ SQUID loop, which is completely suspended after etching. A side-view SEM of a suspended SQUID transmon is shown in Figure 3(a). We compare this device with another that underwent BOE before deposition and no other surface cleaning or etching after deposition. The two qubits were symmetrically arranged inside the same copper cavity to ensure that they experienced a similar background electromagnetic environment. Two separate solenoid coils mounted outside the cavity and aligned with the location of the qubits allowed us to individually control the frequency of each device.

We plot T_1 as a function of qubit frequency for one pair of regular and suspended qubits in Figures 3(b) and 3(c), respectively. For the regular qubit, we find that in addition to a low overall T_1 of $< 10\ \mu\text{s}$, there are sharp dips in the T_1 at a multitude of distinct frequencies. The suspended qubit shows a higher overall T_1 , but also exhibits a few resonant features where the T_1 is drastically reduced. A second pair of qubits measured in the same manner exhibited similar behavior. These observations imply that both types of qubits are affected by the presence of resonant loss channels such as TLS's, as was observed in many previous studies.^{5,25} We observe that the resonant loss channels are less prevalent for the suspended qubit than the regular qubit. However, their presence may explain the variability that we observe in the T_1 measurements of single junction qubits.

The 3D SQUID transmons also allow us to investigate if and how suspension affects their magnetic environments. In particular, many previous works have observed $1/f$ flux noise experienced by several different types of superconducting qubits.^{8–10} It has been proposed that similar to dielectric loss, flux noise can be caused by defects in amorphous surface materials, such as silicon oxide.¹⁹ However, typical measured flux noise levels in SQUIDs have been orders of magnitude higher than estimates based on known sources,

and the origin of this important dephasing mechanism for superconducting qubits remains uncertain.^{9,10,26}

In order to measure the noise power spectral density (PSD) of the qubits, we use the technique demonstrated in Bylander *et al.*²⁶ We measure the response of the qubits to a collection of Carr-Purcell-Meiboom-Gill (CPMG) dynamical decoupling sequences with varying time delays and number of pulses to filter out noise at different frequencies. We can then use this in combination with the measured frequency-flux curves for the qubits to extract the PSD within a range of noise frequencies.²⁶ The results are shown in Figure 3(d). The PSD's include data from two pairs of regular and suspended qubits measured in the same cavity on successive cooldowns. The data from the two pairs of qubits agree very well with each other, indicating that the observed differences between the two types of qubits are not due to sample to sample variations. The flux noise for both qubits exhibits a clear power law dependence with an exponent of $\alpha = 0.81 \pm 0.02$ for the suspended qubit and $\alpha = 0.94 \pm 0.04$ for the regular qubit. Assuming the same power law dependence at lower frequencies, we find the flux noise amplitude at 1 Hz to be $(14.6 \pm 0.7\ \mu\Phi_0)^2$ for the suspended qubit and $(21 \pm 2\ \mu\Phi_0)^2$ for the regular qubit. The different exponents of the two PSD curves result in a slightly higher flux noise estimate at 1 Hz for the regular qubit after extrapolating over many orders of magnitude in frequency. In the measured frequency range, however, the flux noise of the suspended qubits is higher than the regular qubits by a factor of ~ 3 . We also performed the same measurements at the zero-flux points of each qubit and found that the PSD was essentially flat at the level of $10^{-16}\ \Phi_0^2/\text{Hz}$. This suggests that the measured noise in this frequency range is likely to be flux-related and not due to, for example, critical current fluctuations.

While one might expect that removing the substrate from underneath the SQUID loop would decrease the flux noise due to surface spins, our data indicate that the opposite effect occurs in the measured frequency range. It has been suggested that the dominant contributors to flux inside the SQUID loop are spins on the surface of the loop traces.¹⁹ Therefore, removing the silicon surface inside and outside the loop may not have a large effect on the flux noise. On the other hand, DRIE also exposes the bottom surface of the

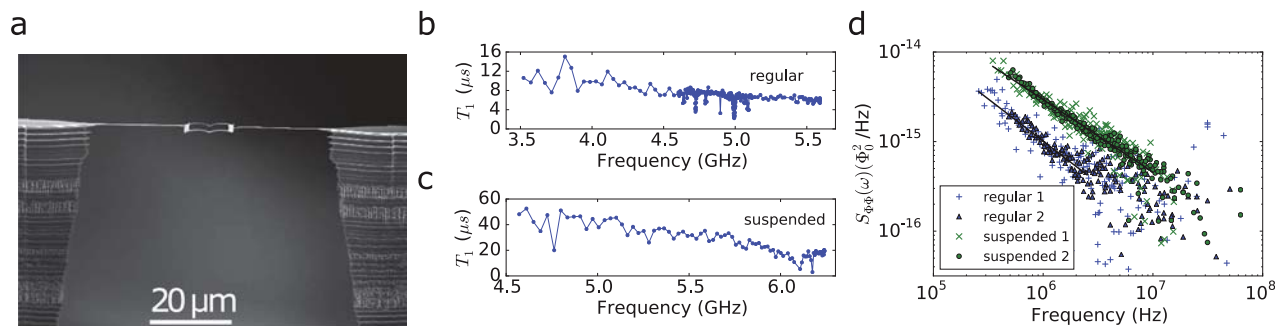


FIG. 3. Flux tunable suspended qubits. (a) Side view SEM image of a suspended SQUID transmon. (b), (c) T_1 vs qubit frequency for regular (b) and suspended (c) qubits. Initial coarsely sampled data revealed many dips in T_1 for the regular qubit, but relatively a few in the suspended qubit. Finer sampled data were taken for the regular qubit to investigate these low- T_1 features, an example of which is shown in the [supplementary materials](#). (d) PSD of flux noise extracted from dynamical decoupling of regular and suspended qubits, each including data from two qubits. Solid lines are fits to the data. The extent of the lines indicates the frequency range in which the data were above the noise floor and therefore included in the fit.

aluminum loop, which forms a layer of amorphous AlO_x in air. Our observations are consistent with the new AlO_x layer having a higher concentration of spins than the aluminum-silicon interface, possibly because most of the SiO_x was removed by BOE prior to deposition. The observation that the flux noise increased by more than a factor of two after etching could suggest that the new AlO_x layer on the bottom surface contains more defects than the top surface. This might be the case given that the top oxide layer was grown in pure oxygen conditions inside the evaporator rather than through exposure to air.²⁷ We emphasize that while this explanation is consistent with our observations, other mechanisms, such as adsorbates on the surface, are also possible.^{28,29} Further investigation would be needed to elucidate the microscopic origins of additional flux noise in suspended qubits.

We have demonstrated that micromachining of silicon substrates is compatible with aluminum Josephson junction qubits. The process results in a reduction of the metal-substrate interface and an improvement of qubit T_1 's. Our results seem to suggest that we are approaching a regime where qubit decay is dominated by other mechanisms such as dielectric loss of the bulk silicon substrate. The loss tangent of “undoped” high-resistivity silicon is not very well known or understood and is likely to be dependent on residual dopants and defects. We speculate that the DRIE technique described here, in combination with higher quality substrates, can result in qubits with even longer lifetimes. In addition, MS and bulk participation ratios can be further reduced by redesigning the qubit, so that the DRIE process suspends larger areas of the device. We emphasize, however, that dielectric loss will eventually become dominated by another material. Even in the limit of a qubit floating in vacuum, there will be dielectric loss due to, for example, oxide on the surface of the metal. Beyond the reduction of dielectric loss, our measurements of flux noise with suspended SQUID transmons is another example of how qubit properties can be altered by changing the geometry of the substrate and the materials present in the environment. We expect that other potential loss mechanisms for circuit QED devices, such as quasiparticles and phonon coupling,^{23,24} will also be affected. Therefore, our process provides a tool for understanding and improving the various aspects involved in the performance of superconducting qubits.

See [supplementary material](#) for additional details on fabrication, simulation, and flux noise analysis.

We thank Luke Burkhardt, Mollie Schwartz, and Michel Devoret for valuable discussions. Facilities use was supported by the Yale SEAS cleanroom, YINQE and NSF MRSEC DMR-1119826. This research was supported by the Army Research Office under Grant No. W911NF-14-1-0011. C.A. acknowledges support from the NSF Graduate Research Fellowship under Grant No. DGE-1122492. Y.Y.G. acknowledges support from an A*STAR NSS Fellowship.

- ¹H. Paik, D. I. Schuster, L. S. Bishop, G. Kirchmair, G. Catelani, A. P. Sears, B. R. Johnson, M. J. Reagor, L. Frunzio, L. I. Glazman, S. M. Girvin, M. H. Devoret, and R. J. Schoelkopf, *Phys. Rev. Lett.* **107**, 240501 (2011).
- ²R. Barends, J. Kelly, A. Megrant, D. Sank, E. Jeffrey, Y. Chen, Y. Yin, B. Chiaro, J. Mutus, C. Neill, P. O'Malley, P. Roushan, J. Wenner, T. C. White, A. N. Cleland, and J. M. Martinis, *Phys. Rev. Lett.* **111**, 080502 (2013).
- ³J. M. Martinis and A. Megrant, e-print [arXiv:1410.5793](#).
- ⁴C. Wang, C. Axline, Y. Y. Gao, T. Brecht, Y. Chu, L. Frunzio, M. H. Devoret, and R. J. Schoelkopf, *Appl. Phys. Lett.* **107**, 162601 (2015).
- ⁵J. M. Martinis, K. B. Cooper, R. McDermott, M. Steffen, M. Ansmann, K. D. Osborn, K. Cicak, S. Oh, D. P. Pappas, R. W. Simmonds, and C. C. Yu, *Phys. Rev. Lett.* **95**, 210503 (2005).
- ⁶J. B. Chang, M. R. Vissers, A. D. Córcoles, M. Sandberg, J. Gao, D. W. Abraham, J. M. Chow, J. M. Gambetta, M. Beth Rothwell, G. A. Keefe, M. Steffen, and D. P. Pappas, *Appl. Phys. Lett.* **103**, 012602 (2013).
- ⁷J. Gao, M. Daal, A. Vayonakis, S. Kumar, J. Zmuidzinas, B. Sadoulet, B. A. Mazin, P. K. Day, and H. G. Leduc, *Appl. Phys. Lett.* **92**, 152505 (2008).
- ⁸F. Yoshihara, K. Harrabi, A. O. Niskanen, Y. Nakamura, and J. S. Tsai, *Phys. Rev. Lett.* **97**, 167001 (2006).
- ⁹R. C. Bialczak, R. McDermott, M. Ansmann, M. Hofheinz, N. Katz, E. Lucero, M. Neeley, A. D. O'Connell, H. Wang, A. N. Cleland, and J. M. Martinis, *Phys. Rev. Lett.* **99**, 187006 (2007).
- ¹⁰S. M. Anton, J. S. Birenbaum, S. R. O'Kelley, V. Bolkhovskiy, D. A. Braje, G. Fitch, M. Neeley, G. C. Hilton, H. M. Cho, K. D. Irwin, F. C. Wellstood, W. D. Oliver, A. Shnirman, and J. Clarke, *Phys. Rev. Lett.* **110**, 147002 (2013).
- ¹¹A. D. O'Connell, M. Ansmann, R. C. Bialczak, M. Hofheinz, N. Katz, E. Lucero, C. McKenney, M. Neeley, H. Wang, E. M. Weig, A. N. Cleland, and J. M. Martinis, *Appl. Phys. Lett.* **92**, 112903 (2008).
- ¹²J. M. Gambetta, C. E. Murray, Y. K. K. Fung, D. T. McClure, O. Dial, W. Shanks, J. Sleight, and M. Steffen, e-print [arXiv:1605.08009](#).
- ¹³G. T. A. Kovacs, N. I. Maluf, and K. E. Petersen, *Proc. IEEE* **86**, 1536 (1998).
- ¹⁴T. Brecht, W. Pfaff, C. Wang, Y. Chu, L. Frunzio, M. H. Devoret, and R. J. Schoelkopf, *NPJ Quantum Inf.* **2**, 16002 (2015).
- ¹⁵T. Brecht, M. Reagor, Y. Chu, W. Pfaff, C. Wang, L. Frunzio, M. H. Devoret, and R. J. Schoelkopf, *Appl. Phys. Lett.* **107**, 192603 (2015).
- ¹⁶A. Bruno, G. de Lange, S. Asaad, K. L. van der Enden, N. K. Langford, and L. DiCarlo, *Appl. Phys. Lett.* **106**, 182601 (2015).
- ¹⁷R. Barends, N. Vercruyssen, A. Endo, P. J. de Visser, T. Zijlstra, T. M. Klapwijk, and J. J. A. Baselmans, *Appl. Phys. Lett.* **97**, 033507 (2010).
- ¹⁸M. V. Schickfus and S. Hunklinger, *Phys. Lett. A* **64**, 144 (1977).
- ¹⁹R. H. Koch, D. P. DiVincenzo, and J. Clarke, *Phys. Rev. Lett.* **98**, 267003 (2007).
- ²⁰F. Laermer and A. Schilp, “Method of anisotropically etching silicon,” U.S. patent 5501893 (1996).
- ²¹G. J. Dolan, *Appl. Phys. Lett.* **31**, 337 (1977).
- ²²D. H. Slichter, “Quantum jumps and measurement backaction in a superconducting qubit,” Ph.D. thesis, University of California, Berkeley, 2011.
- ²³G. Catelani, R. J. Schoelkopf, M. H. Devoret, and L. I. Glazman, *Phys. Rev. B* **84**, 064517 (2011).
- ²⁴L. B. Ioffe, V. B. Geshkenbein, C. Helm, and G. Blatter, *Phys. Rev. Lett.* **93**, 057001 (2004).
- ²⁵J. Lisenfeld, G. J. Grabovskij, C. Müller, J. H. Cole, G. Weiss, and A. V. Ustinov, *Nat. Commun.* **6**, 6182 (2015).
- ²⁶J. Bylander, S. Gustavsson, F. Yan, F. Yoshihara, K. Harrabi, G. Fitch, D. G. Cory, Y. Nakamura, J.-S. Tsai, and W. D. Oliver, *Nat. Phys.* **7**, 565 (2011).
- ²⁷J. M. Schneider, A. Anders, B. Hjärvarsson, I. Petrov, K. Macák, U. Helmerson, and J.-E. Sundgren, *Appl. Phys. Lett.* **74**, 200 (1999).
- ²⁸P. Kumar, S. Sendelbach, M. A. Beck, J. W. Freeland, Z. Wang, H. Wang, C. C. Yu, R. Q. Wu, D. P. Pappas, and R. McDermott, e-print [arXiv:1604.00877](#).
- ²⁹D. Lee, J. L. DuBois, and V. Lordi, *Phys. Rev. Lett.* **112**, 017001 (2014).